Supplement of Atmos. Chem. Phys., 25, 3905–3918, 2025
https://doi.org/10.5194/acp-25-3905-2025-supplement


Atmospheric Chemistry and Physics
Open Access
EGU

*Supplement of*

# The impact of organic nitrates on summer ozone formation in Shanghai, China

**Chunmeng Li et al.**

*Correspondence to:* Xiaorui Chen (chenxr95@mail.sysu.edu.cn) and Keding Lu (k.lu@pku.edu.cn)

**S1. The description of mechanistic uptake in Zare Mechanism**

Firstly, the BVOCs oxidized by OH and $NO_3$ have been refined and supplemented, and the various reactions between $RO_2$ and NO, as well as the conversion between ROx, have been updated to ensure the applicability in high/low $NO_x$ environments (Zare et al., 2018). For isoprene, the mechanism update contains refinements for oxidation reactions initiated by OH and $NO_3$. For monoterpenes, the relevant updates mainly include reaction rate constants for API and $NO_3$ and API is represented by α-pinene and β-pinene. Under the above updates, ANs contain a total of 24 species, of which 4 are secondarily generated. For the deposition, except the deposition rates of $R_4NO$ (C4 nitrooxycarbonyl hydroperoxide), PROPNN (propanone nitrate), and TONIH (C10 nitrooxy hydroperoxide) were set to 1.3±0.6, 1.7±0.6 and 0.8±0.4 cm/s, respectively, the rest were set to 1.5 cm/s according to ISOPN (hydroxy isoprene nitrates) (Nguyen et al., 2015). The uptake of ANs was quantified by speciation parameterization, and key parameters mainly included uptake coefficients, aerosol surface areas, and molecular motion rates. The uptake coefficients are distributed in the range of 0.005 - 0.01 according to the ANs species, the molecular speed is valued by ISO, and the aerosol surface area concentration is parameterized according to the empirical formula through the mass concentration of $PM_{2.5}$ (Wang et al., 2021).

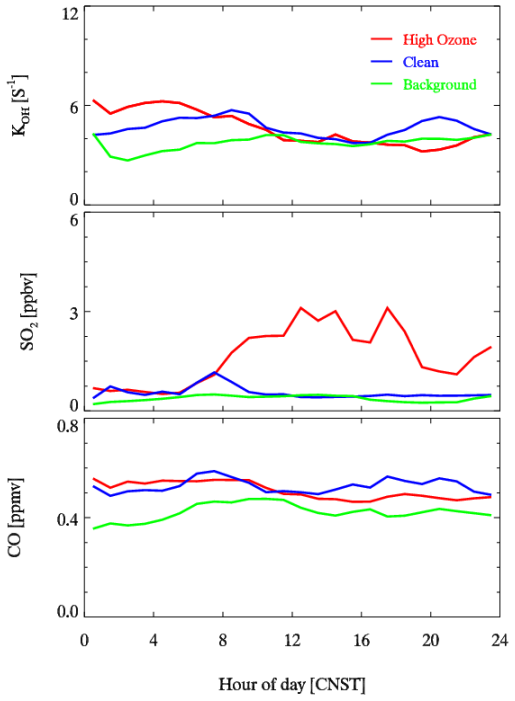


**Figure S1.** Mean diurnal profiles of VOC reactivity ($K_{OH}$), $SO_2$ and CO during different observation periods.

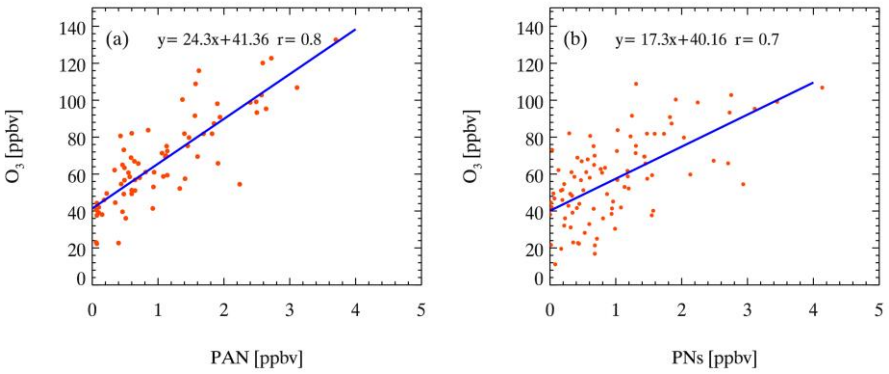


**Figure S2.** Correlation analyses of ozone and PAN (a) or PNs (B) during the Shanghai campaign.

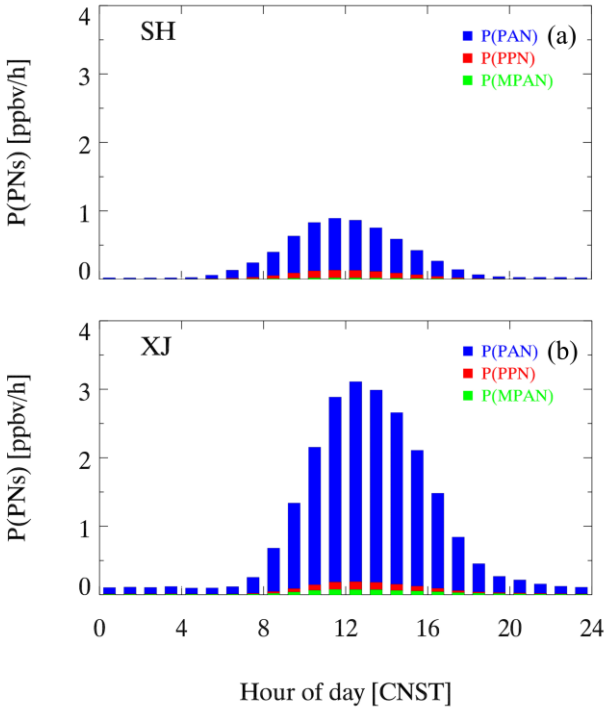


**Figure S3.** The mean diurnal production rate of PNs (P(PNs)) calculated by kinetic calculation method during Shanghai campaign (a) and Shanghai campaign (b). The kinetic calculation method is to calculate the total production potential of PAN, MPAN and PPN, which is determined by VOCs distribution, reaction rate constant and OH concentration, detailed in previous study (Li et al., 2023).

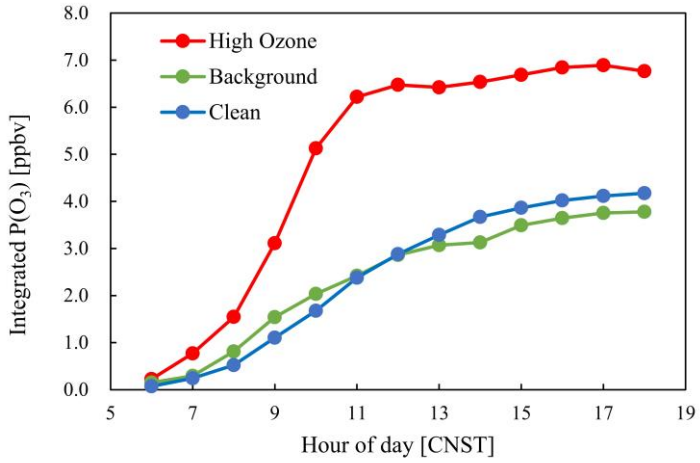


**Figure S4.** The integrated $P(O_3)$ changes constrained by PNs photochemistry during different observation periods.

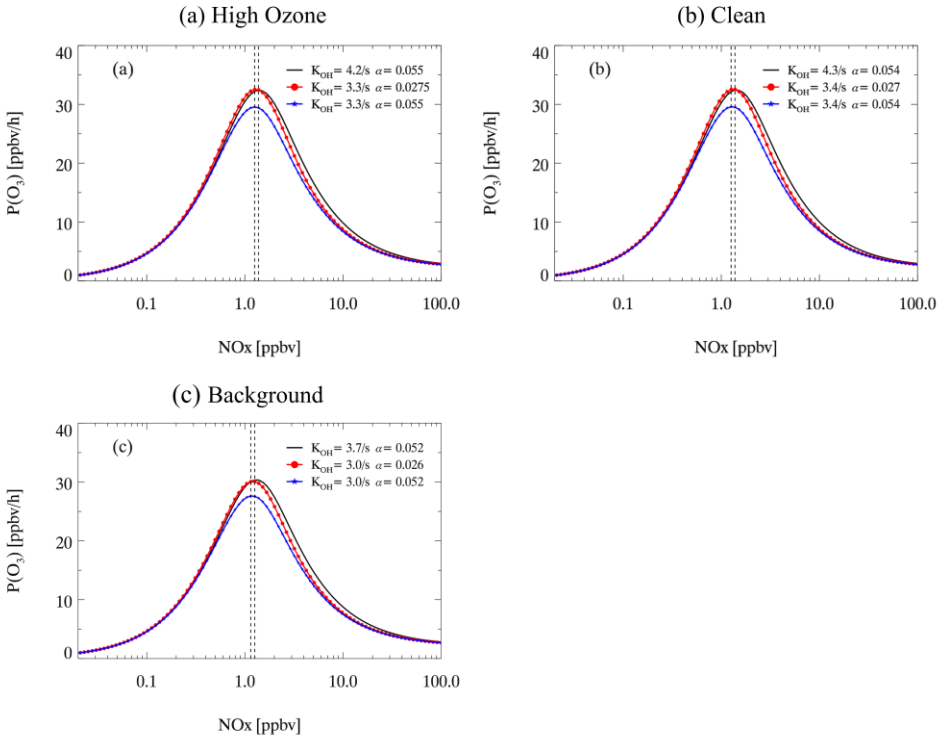


**Figure S5.** The ozone production rate ($P(O_3)$) varies as a function of $NO_x$ under different VOC-$NO_x$ regimes during Shanghai campaign: (a) under measured parameters during high ozone period; (b) during the clean period; (c) during the background period. The solid line shows the mean $K_{OH}$ with effective α; the red dot line shows a 20% reduction in $K_{OH}$ with a 50% reduction in α; the blue dot line shows a 20% reduction in $K_{OH}$ with no change in α. Dash lines show the turning point in different cases.

**Table S1.** The species of ANs precursors observed during the Shanghai campaign with corresponding branching ratio and averages of concentration (ppbv).

| Species | Branching ratio | Concentration |
|---|---|---|
| ethane | 0.019 | 2.858 |
| propane | 0.036 | 2.388 |
| n_butane | 0.077 | 1.115 |
| n_pentane | 0.105 | 0.384 |
| iso_butane | 0.096 | 0.851 |
| iso_Pentane | 0.007 | 0.522 |
| _2_2_Dimethylbutane | 0.152 | 0.016 |
| cyclopentane | 0.045 | 0.110 |
| _2_Methylpentane | 0.097 | 0.086 |
| _3_Methylpentane | 0.109 | 0.113 |
| _2_2_4_trimethylpentane | 0.14 | 0.028 |
| methylcyclopentane | 0.14 | 0.096 |
| n_hexane | 0.141 | 1.052 |
| Cyclohexane | 0.16 | 0.144 |
| methylcyclohexane | 0.17 | 0.048 |
| n_heptane | 0.178 | 0.133 |
| n_octane | 0.226 | 0.072 |
| n_nonane | 0.393 | 0.033 |
| n_decane | 0.417 | 0.035 |
| ethene | 0.0086 | 1.169 |
| propene | 0.015 | 0.258 |
| _1_butene | 0.025 | 0.077 |
| _2_methyl_1_butene | 0.02 | 0.009 |
| _3_methyl_1_butene | 0.059 | 0.002 |
| _2_methyl_2_butene | 0.034 | 0.004 |
| trans_2_butene | 0.034 | 0.049 |
| cis_2_butene | 0.034 | 0.104 |
| _1_pentene | 0.059 | 0.022 |
| trans_2_pentene | 0.064 | 0.012 |
| cis_2_pentene | 0.064 | 0.017 |
| _1_3_butadiene | 0.007 | 0.018 |
| _1_hexene | 0.055 | 0.010 |
| isoprene | 0.07 | 0.154 |
| methacrolein | 0.15 | 0.069 |
| methyl_vinyl_ketone | 0.11 | 0.144 |
| ALPHA_PINENE | 0.18 | 0.008 |
| BETA_PINENE | 0.24 | 0.015 |
| D_LIMONENE | 0.23 | 0.010 |
| Benzene | 0.034 | 0.235 |

| | | |
|---|---|---|
| p_diethylbenzene | 0.093 | 0.017 |
| toluene | 0.029 | 0.634 |
| o_Ethyltoluene | 0.106 | 0.014 |
| m_Ethyltoluene | 0.094 | 0.015 |
| p_Ethyltoluene | 0.137 | 0.009 |
| o_xylene | 0.081 | 0.139 |
| M_P_xylenes | 0.074 | 0.311 |
| ethylbenzene | 0.072 | 0.190 |
| _1_3_5_trimethylbenzene | 0.081 | 0.008 |
| _1_2_4_trimethylbenzene | 0.105 | 0.021 |
| _1_2_3_trimethylbenzene | 0.119 | 0.011 |
| iso_propylbenzene | 0.11 | 0.010 |
| Weighting averages | 0.053 | / |

## References

Li, C., Wang, H., Chen, X., Zhai, T., Ma, X., Yang, X., Chen, S., Li, X., Zeng, L., and Lu, K.: Observation and modeling of organic nitrates on a suburban site in southwest China, Sci. Total Environ., 859, 10.1016/j.scitotenv.2022.160287, 2023.

Nguyen, T. B., Crounse, J. D., Teng, A. P., St. Clair, J. M., Paulot, F., Wolfe, G. M., and Wennberg, P. O.: Rapid deposition of oxidized biogenic compounds to a temperate forest, Proc. Natl. Acad. Sci. U. S. A., 112, E392-E401, 10.1073/pnas.1418702112, 2015.

Wang, H., Lu, K., Chen, S., Li, X., Zeng, L., Hu, M., and Zhang, Y.: Characterizing nitrate radical budget trends in Beijing during 2013–2019, Science of The Total Environment, 795, 10.1016/j.scitotenv.2021.148869, 2021.

Zare, A., Romer, P. S., Tran, N., Keutsch, F. N., Skog, K., and Cohen, R. C.: A comprehensive organic nitrate chemistry: insights into the lifetime of atmospheric organic nitrates, Atmos. Chem. Phys., 18, 15419-15436, 10.5194/acp-18-15419-2018, 2018.